CYCLIC TRIAXIAL TEST TO MEASURE STRAIN-DEPENDENT SHEAR

MODULUS OF UNSATURATED SAND

By: Majid Ghayoomi, Ph.D.¹, Associate Member ASCE

Ganna Suprunenko²

and Morteza Mirshekari³

Abstract: Dynamic shear modulus plays an important role in seismic assessment of geotechnical systems. Changes in degree of water saturation influence dynamic soil properties due to the presence of matric suction. This paper describes the modification of a suction-controlled cyclic triaxial apparatus to investigate strain-dependent shear modulus of unsaturated soils. Several strain-controlled and stress-controlled cyclic triaxial tests were performed on a clean sand with various degrees of saturation. Suction in unsaturated sands increased the shear modulus in comparison with the ones in dry and saturated conditions for different shear strain levels, with a peak modulus in higher suction levels. Also, shear modulus decreased by increasing the shear strain for specimens with similar matric suction. The normalized shear moduli of the unsaturated sand specimens followed a similar trend to the ones predicted by the available empirical shear modulus reduction functions, but showing lower normalized shear modulus values. Modulus reduction ratios of unsaturated sands shifted up as a result of higher effective stress and suction-induced stiffness. These trends were consistent for both strain- and stress-controlled tests.

¹ Assistant Professor, University of New Hampshire, Department of Civil and Environmental Engineering, 33 Academic Way, Durham, NH 03824, majid.ghayoomi@unh.edu.

² Graduate Research Assistant, University of New Hampshire, Department of Civil and Environmental Engineering, 33 Academic Way, Durham, NH 03824.

³ Graduate Research Assistant, University of New Hampshire, Department of Civil and Environmental Engineering, 33 Academic Way, Durham, NH 03824

INTRODUCTION

Dynamic soil properties are key parameters in seismic design and performance of geotechnical systems. Accurate estimation of dynamic shear modulus (G) is crucial in proper evaluation of soil response to dynamic loads such as earthquakes, blasts, road and rail traffic, wind, and ocean waves. Previous studies indicated that the dynamic shear modulus follows a nonlinear trend where its value decreases as the induced strain level increases (Hardin and Drnevich 1972).

The small-strain or the maximum shear modulus (i.e. G_0 or G_{max} , respectively) occurs at small shear strains (γ < 10⁻⁴ %; Kramer 1996). Using the data from laboratory experiments (e.g. Resonant Column or Bender Element tests) or from geophysical methods (e.g. seismic wave methods) several empirical equations have been proposed to estimate G_0 (Seed and Idriss 1970, Hardin and Drnevich 1972). These equations include the effects of void ratio or density, stress history, plasticity index, soil type, and mean effective stress, and they follow a general format presented by Hardin and black (1969), shown in Equation 1.

$$G_0 = A(OCR)^K f(e) P_a^{1-n} p'^n$$
(1)

where A and n are fitting parameters that vary for different soils, OCR is the over-consolidation ratio, p' is the mean effective stress, P_a is the atmospheric pressure, K is the hardening parameter related to the plasticity index of soils PI, and f(e) is a function of void ratio.

Strain-dependent shear moduli are presented using shear modulus reduction functions or curves. These functions originated from a standard nonlinear hyperbolic model (Kondner and Zelasko 1963), and later, they were modified to more sophisticated

empirical equations (Hardin and Drnevich 1972, Darendeli 2001). Torsional shear test, cyclic triaxial test, and cyclic simple shear test are among the experimental procedures used for this purpose. The general form of a hyperbolic shear modulus reduction function is presented in Equation 2.

$$\frac{G}{G_0} = \frac{1}{1 + \frac{\gamma}{\gamma_r}} \tag{2}$$

where G is the strain-dependent shear modulus, γ is the shear strain, and γ_r is the reference shear strain corresponding to $G/G_0=0.5$.

49

50

51

52

53

54

55

56

57

58

59

60

61

62

63

64

Recent advancements in unsaturated soil mechanics have revealed the clear influence of degree of water saturation on dynamic properties of soils (Khosravi et al. 2010, Ghayoomi and McCartney 2011, Khosravi et al. 2016). This is due to the presence of interparticle suction forces that change the effective stresses in soils (Khalili et al. 2004), and in turn, the mechanical response. Thus, soils with different degrees of saturation differ in stiffness, and consequently results in different dynamic response, seismic compression, and pore water pressure generation and dissipation in geotechnical system (Ghayoomi et al. 2013, Ghayoomi and Mirshekari 2014, Cary and Zapata 2016). Experimental difficulties, such as direct measurement and control of matric suction, hindered investigation of dynamic behavior of unsaturated soils. As yet researchers have increasingly explored the effect of degree of saturation on dynamic soil modulus and damping. However, they mostly focused on small-strain shear modulus for various suction values or degrees of saturation using bender element or resonant column tests (Wu et al. 1984, Qian et al. 1991, Marinho et al. 1995, Cho and Santamarina 2001, Mancuso et al. 2002, Mendoza et al. 2005, Alramahi et al. 2007, Ng et al. 2009, Khosravi et al. 2010, Ghayoomi and McCartney 2011, Hoyos et al. 2015). In addition, in some recent studies, researchers investigated the effect of suction on strain-dependent shear modulus, soil volume change, stress path, pore pressure, and drainage condition in cyclic triaxial system (Cui et al. 2007, Craciun and Lo 2010, Biglari et al. 2011, Kimoto et al. 2011, Cary and Zapata 2016). However, the effect of the degree of saturation on soil stiffness for medium to large strain levels still requires further examination, especially when it relates to dynamic analysis. Recently, Biglari et al. (2011) used cyclic triaxial test to show the modulus reduction in unsaturated soils. However, the results were not compared with available modulus reduction formulas to check whether they are consistent with the predicted range regardless of the degree of saturation or testing method. In addition, changes in the matric suction during loading cycles and consequent modulus alterations were not reported. The potential application of such consistent modulus reduction function could be in soil-foundation interaction problems dealing with shallow unsaturated soils, seismic site response analysis with variable degree of saturation profile, or the deformation of roads and pavement structures due to the fluctuation of water content in the soil layers.

This paper explains the modification and implementation of a cyclic triaxial testing system for dynamic loading in controlled suction condition. Changes to the system and testing procedures are presented followed by verification data. The shear modulus reduction data for dry, saturated, and unsaturated soils are presented and compared. Then, the normalized modulus reduction ratios are compared to available shear modulus reduction curves. In addition, the effect of suction (degree of saturation) on measured modulus and the extent of its effect are presented and discussed. Further, the success of drained or constant-suction triaxial tests on unsaturated sand specimens is examined by monitoring the pore pressure and shear modulus throughout cyclic tests. The objectives

of the paper are threefold: 1) show the development process and verification of a suction controlled-triaxial system; 2) demonstrate how suction affects shear modulus; 3) examine the consistency of the measured data and other available modulus reduction functions using an effective stress-based approach.

Background

89

90

91

92

93

94

95

96

97

98

99

100

101

102

103

104

105

106

107

108

109

110

111

Dynamic Shear Modulus

Dynamic shear modulus represents soil stiffness in shear and can be calculated from the slope of shear stress-strain curve obtained from cyclic tests. Parameters such as strain level, loading pattern, intensity, overburden pressure, and water content can affect these properties (Seed and Idriss 1970, Kramer 1996). Using any element scale dynamic test, a hysteresis loop is formed by plotting stress versus strain path during cyclic loading, as shown in Figure 1(a). This loop is used to estimate the dynamic properties of geomaterial, i.e. shear modulus and damping. The backbone curve, shown in Figure 1(b), which forms a basis for the stress-strain response, is defined by two major values: 1) the steepest slope at small strain (G_0) and the asymptote at large strain (i.e. shear strength, τ_{max}). Secant shear modulus (G_{sec}) (called shear modulus, G, in this paper) at any given strain level is defined by the slope of the line connecting the origin to the point of interest on the backbone curve $(G = G_{sec} = \frac{\tau}{v})$ and decreases by increasing the shear strain. Although G₀-slope is visible in the hysteresis loops obtained from cyclic triaxial tests, but it is rarely calculated due to the low accuracy of cyclic triaxial system in small strain ranges. However, using apparatuses such as resonant column device or bender element system, one can determine G₀. For example,

Seed and Idriss (1970) proposed the following empirical equation for G₀ of sands.

$$G_0 = 1000K_{2,\text{max}}(\sigma'_{\text{m}})^{1/2}$$
(3)

where $K_{2,max}$ is related to the soil relative density or void ratio and σ'_m is the mean effective stress in psf.

The strain-dependent shear modulus declines as the shear strain amplitude rises. In geotechnical engineering practice this reduction is shown by the normalized modulus reduction curves, i.e. the ratio of the strain-dependent shear modulus to the small-strain shear modulus (G/G_0), shown in Figure 2. Hardin and Drnevich (1972) used a hyperbolic function to present the shear modulus reduction curve, as in Equation 2. They estimated the reference shear strain, γ_r , using the following equation (shown in Figure 1(b)).

$$\gamma_{\rm r} = \frac{\tau_{\rm max}}{G_0} \tag{4}$$

where τ_{max} is the shear stress at failure that depends on the initial state of stress in the soil. Hardin and Drnevich (1972) adapted the concept of failure in pure shear and calculated the shear stress at failure using Equation 5.

$$\tau_{\text{max}} = \left\{ \left[\frac{1 + K_0}{2} \sigma_{\text{v}}' \sin \varphi' + c' \cos \varphi' \right]^2 - \left[\frac{1 - K_0}{2} \sigma_{\text{v}}' \right]^2 \right\}^{1/2}$$
 (5)

where K_0 is the coefficient of lateral earth pressure at rest, c' and ϕ' are the static strength parameters ($c' \sim 0$ for clean sand), σ'_v is the vertical effective stress. However, one can determine the shear strength (i.e. stress at failure) under triaxial loading condition as in Equation 6.

$$\tau_{\text{max}} = \frac{\sigma_c(\tan^2\left(45 + \frac{\varphi'}{2}\right) - 1)}{2}\cos\left(\varphi'\right) \tag{6}$$

where σ_c is the cell confining pressure.

114

115

116

117

118

Further, Darendeli (2001) and Menq (2003) modified the basic hyperbolic form by adding a power "a" to the shear strain ratio, as in Equation 7. Based on a set of torsional shear and resonant column test data, they proposed the following empirical correlations to estimate γ_r and a.

$$\frac{G}{G_{\text{max}}} = \frac{1}{1 + \left(\frac{\gamma}{\gamma_r}\right)^a}$$

$$\gamma_r = 0.12 \cdot C_u^{-0.6} \cdot \left(\frac{\sigma'_m}{P_a}\right)^{0.5 \cdot C_u^{-0.15}}$$

$$a = 0.86 + 0.1 \cdot \log\left(\frac{\sigma'_m}{P_a}\right)$$
(7)

where C_u is the coefficient of uniformity, P_a is the atmospheric pressure, and σ_m' is the mean effective stress. Considering the proposed equations for small-strain shear modulus and shear modulus reduction functions, one can infer that the effective stress could significantly influences the dynamic soil modulus.

Effective Stress in Unsaturated Soils

Soils in nature tend to be fully saturated below the water table and become unsaturated above the ground water table. In unsaturated soils, the air-water interface causes additional inter-particle suction that depends on soil type and grain size distribution (Lu and Likos 2006). Soil-Water Retention Curve (SWRC) represents a constitutive function between matric suction and degree of water saturation.

Negative pore water pressure in unsaturated soils results in tensile forces that will increase the effective stress. Proposing an effective stress formula consistent for dry, unsaturated, and saturated soils has been the area of research for several years. It was initiated by Bishop's effective stress equation (Bishop 1959).

$$\sigma' = (\sigma - u_a) + \chi(u_a - u_w) \tag{8}$$

where σ' is the effective stress, σ is the total stress, u_a is the pore air pressure, u_w is the pore water pressure, $u_a - u_w$ is the matric suction, and χ is the effective stress parameter ranging from 0 to 1. The net normal stress is represented by the first term in the equation, while the second term, i.e. $\chi(u_a - u_w)$, is called the suction stress (Lu et al. 2010). Among many proposed formulas Lu et al. (2010) incorporated the concept of suction stress and van Genuchten's (1980) SWRC fitting parameters (α and n) to estimate the effective stress in unsaturated soils as a function of suction and net normal stress:

$$\sigma' = \sigma - u_a + \frac{u_a - u_w}{(1 + [\alpha(u_a - u_w)]^n)^{1 - \frac{1}{n}}}$$
(9)

Estimating dynamic shear modulus using the effective stress formula in Equation 9 regardless of the degree of saturation will be valuable in seismic analysis of unsaturated soil layers. For example, Ghayoomi and McCartney (2011) integrated Equation 9 and available empirical relations for dry sand to estimate G_0 of sands with various degrees of saturation. The predicted values were very close to the measured G_0 values using resonant column and bender element tests. Similar application of this equation in strain-dependent shear modulus functions, however, requires further experiments and analysis. In addition, proven validity of such consistent formula would imply that suction impacts the shear modulus indirectly through the effective stress.

Experimental Procedures

Cyclic Triaxial System

A GCTS cyclic triaxial system was implemented to perform static and dynamic tests. The pressure control panel PCP-3000 was operated by a hydraulic oil pump capable of introducing 1000 kPa pressure. Cyclic load was applied through a hydraulic servo valve

with different wave forms with frequencies up to 10 Hz. Actuator movement, water pressure inside the specimen, and cell pressure can be controlled both manually using the pressure panel or through the integrated CATS software that operates GCTS SCON-1000 digital system controller and data acquisition system with a sampling frequency of 100 Hz. Different stages of triaxial testing such as saturation, consolidation, and loading can be automatically controlled and programmed as needed. A schematic of the triaxial system is shown in Figure 3. Due to the system compliance constraints, only axial strains higher than 0.01% was obtainable using this experimental setup. Thus, the testing strain range focused on medium to large strain levels.

Suction Control System

The most common technique for controlling suction in the laboratory is the axis translation technique (Hilf 1956). The procedure includes water pressure control through a saturated interface, i.e. saturated High Air Entry Value (HAEV) disc, and artificial increase of the air pressure in the soil sample. This technique yields results even at elevated suction levels, as well as nearly saturated conditions. The difference in pressure at the bottom (water) and at the top (air) of the specimen is measured with a differential pressure transducer representing soil suction. Because the pressures are induced at the boundaries, the system needs to equilibrate throughout the soil to give reasonably uniform matric suction. In order to control the volume of displaced water from the specimen and to monitor the equilibrated suction, a feedback loop is required.

The GCTS triaxial system was improved for testing soils with different levels of saturation. For matric suction application and monitoring, the bottom platen was modified by installing a ½ bar High Air Entry Value (HAEV) ceramic disc glued using LORD AP-134 epoxy adhesive. Water flow is supported by two grooves underneath the

disc to increase the area of water penetration. Precise control of the flow rate and pore water pressure was achieved through DigiFlow pump developed by the GEOTAC company. The design of this equipment is very similar to a syringe that induces various water flows to the specimen. A solid steel reservoir with a capacity of 80 mL was filled with water and connected to a circular piston. By operating the stepper motor, the piston would slowly move with a threaded rod into the reservoir and induce the flow to the specimen. This flow pump is capable of applying flow rates in the range of $3.96 \cdot 10^{-6}$ to $7.92 \cdot 10^{-12}$ m³/s. A pressure sensor with a capacity of 690 kPa was attached to the flow pump.

The pump can operate in volume- or pressure-control modes and allows selecting the rate of flow, total volume, and direction. Pressure control allows instant application or ramping that is particularly useful for unsaturated soil testing to prevent damage of the high air entry value disk. In these set of tests, the valve to the top of the specimen was kept open to the atmosphere to maintain atmospheric pressure, so the matric suction was only controlled by the negative pressure at the bottom of the specimen. For a more accurate and independent measurement of matric suction, an additional Validyne Differential Pressure Transducer (DPT) was added to the system measuring the difference in pressure on the top and the bottom of the specimen.

After setting the target suction pressure, the pump started withdrawing water from the bottom of the specimen through the HAEV ceramic disc. Upon reaching the desirable suction value the pump stopped. The pump restarted automatically when suction value at the bottom of the specimen was lower than the target value, due to water movement from the top to the bottom of the specimen. For each value of matric suction the system was left to equilibrate until the volume of withdrawing water was less than 0.002 mL/min,

which may take up to 12 hours for sand. The volume of withdrawn water was recorded at each step. This procedure was repeated several times with an increment of 1 kPa in matric suction in order to build a complete SWRC graph.

Material

F-75 Ottawa sand, a fine grained, uniformly distributed silica sand was used in this study. The grain size distribution of this sand is shown in Figure 4, and the physical properties of the material are listed in Table 1. The specimens were prepared at a relative density of 45% representing loosely packed sand. A set of static triaxial tests on dry sand was performed to estimate the soil friction angle and Poisson's ratio. The Poisson's ratio was comparable with values obtained from an empirical relation by Seed and Duncan (1986) (Table 1).

The SWRC for unsaturated F-75 Ottawa sand was obtained using the developed system, as described above and shown in Figure 5. The SWRC was compared with the curves from previous investigations (Ghayoomi et al. 2011, Mirshekari and Ghayoomi 2015), and van Genuchten fitting parameters were estimated (listed in Table 1). Although the sand was poorly graded it was fine enough to retain water up to about 10 kPa of suction.

Testing Procedure

The sand specimens were prepared using dry pluviation (sand raining) method. Except for the dry tests, all the specimens were saturated by flushing de-aired water from the bottom to the top followed by back-pressure saturation until a B-value higher than 0.95 was achieved. For saturated specimens the pore pressure was kept constant and the

cell pressure was increased to reach the target effective stresses of 50 kPa. For testing unsaturated soils, the pore pressure was decreased to zero with reference to the middle of the specimen while the cell pressure was set to 50 kPa. Then, the target suction value was applied through the pump until the system equilibrated. This approach is similar to a tensiometric suction control method, although both tensiometric and axis translation techniques follow the same concept.

Dynamic loads were applied using 10 cycles of sinusoidal deviator strain or stress with a frequency of 1 Hz. Specimens were loaded with an initial seating stress in stress-controlled tests corresponding to equivalent initial seating strain in strain-controlled tests. The purpose of the seating stress or strain was to avoid tension in the specimen during cyclic loading. Single-amplitude deviator axial strain of 0.01, 0.02, 0.05, 0.1, 0.2, and 0.5 % and single-amplitude deviator axial stress of 40, 60, and 80 kPa were applied sequentially in strain- and stress-controlled tests, respectively, listed in Table 2. Consecutive tests with different deviator strain or stress levels were performed on dry, fully saturated, and unsaturated sands with 2.5, 3, 3.5, 4.5, 6, and 10 kPa suction. Adequate time gaps between the tests on one specimen were scheduled to re-equilibrate the pore pressure or suction.

The tests were intended to be performed in fully drained condition, i.e. constant pore pressure or constant suction, by keeping the drainage valve open to the pump with continuous pressure application. However, relative fast loading prevented a fully drained condition where some excess pore water pressure was generated. This so-called "partially drained" condition is very similar to the field condition during earthquake loads and physical modeling experiments (Dashti et al. 2011). Thus, the change in water pressure was carefully considered in data reduction process and shear modulus calculation.

Data Analysis Methods

After completion of the cyclic tests, hysteresis loops were plotted using the deviator axial stress-strain data. Young's modulus was determined by calculating the slope of the axial stress-strain hysteresis loop, as in Equation 10.

$$E = \frac{\Delta \sigma_{\rm d}}{\Delta \varepsilon_{\rm a}} \tag{10}$$

where $\Delta \sigma_d$ is the amplitude of deviator stress and $\Delta \epsilon_a$ is the amplitude of axial strain. Kokusho (1980) performed a series of cyclic triaxial tests and stated that shear modulus for wide strain rate can be calculated from Young's modulus using the following equation

$$G = \frac{E}{2 \cdot (1 + \nu)} \tag{11}$$

where E is Young's modulus and ν is Poisson's ratio. An average Poisson's ratio was used in this equation, simulating a simplified isotropic linear behavior, which was similarly implemented by other researchers (e.g. Georgiannou et al. 1991, and El Mohtar et al. 2013). The average Poisson's ratio measured from the static test and also estimated from the empirical relation was used in this study. Given the shear modulus as the shear stress to strain ratio, $G = \frac{\Delta \tau}{\Delta \gamma}$, the following relationship was implemented in the analysis to calculate the induced shear strain.

$$\Delta \gamma = \Delta \varepsilon_{\rm a} \cdot (1 + \nu) \tag{12}$$

The secant shear modulus was determined using the slope of the line that connects the two ends of the loop (an example is shown in Figure 6 (a)). Except for the cases where a significant soil softening or hardening occurred, the average value of all consecutive loops was considered for further analysis. In large strain tests soil experienced small permanent deformations that caused soil hardening (an example shown in Figure 6 (b)). Further, due

to the partial drainage phenomenon explained above, excess pore pressure was generated during large strain cyclic tests on saturated and unsaturated tests resulted in soil softening (an example is shown in Figure 6 (c)). To reduce these adverse effects in such tests, only first loop with minimal permanent deformation or excess pore pressure was considered in the modulus calculation.

Figure 7, for example, demonstrates the variations of negative pore water pressure (i.e. suction) of unsaturated sand with 2.5 kPa suction, measured using the DPT, after cycles of dynamic loading with 0.2% and 0.5% axial strains, respectively. The maximum recorded change of suction after the first cycle of dynamic test was less than 6 %, which led to a minimal change in effective stress. As the cyclic loading generates excess water pressure, simultaneously, the pump tries to equilibrate suction (i.e. reduce the pore pressure). Thus, the pore pressure variation follows a non-uniform pattern. Although the system could not perfectly represent a drained condition, the partially drained behavior, in nature, is close to what happens in field conditions.

The observed changes in matric suction during cycles of dynamic loading caused variations in the measured shear moduli throughout the cyclic tests. This is illustrated in Figure 8 for two tests with 0.2 and 0.5% axial strains on specimens with 2.5 kPa suction, for which the suction variations were shown in Figures 7. Similarly, the modulus followed a nonlinear pattern due to the simultaneous effects of fast dynamic loads that led to increase in pore pressure and the continuous suction adjustment by the pump that dissipated the excess pore pressure. However, the change in shear modulus may not be fully correlated with the matric suction fluctuations as dynamically-induced permanent deformation could also change the relative density resulting in material hardening in

certain circumstances. Overall, for cases with significant modulus variations only the shear modulus of the first cycle was considered for the following analysis.

Experimental Results and discussion

Effect of Degree of Saturation (Suction) on Shear Modulus

In order to demonstrate the effect of suction or the degree of saturation on shear modulus of unsaturated soils, strain-controlled cyclic triaxial tests with various suction (degree of saturation) levels were performed. Then, the shear modulus and shear strain were calculated from the Young's modulus and axial strain using Equations 11 and 12, respectively. Plots in Figure 9(a) show the changes of shear modulus with the degree of saturation in tests with 0.14%, 0.28%, and 0.69% shear strain. These shear strain levels correspond to 0.1%, 0.2%, and 0.5% axial strain values. Higher shear modulus values were measured for unsaturated sands comparing with those of dry and saturated sands under the same strain level as shown in Figure 9(a). This verifies the stiffer response of unsaturated sand due to the presence of inter-particle suction stresses. To better visualize this effect shear modulus variations were plotted against the suction, related to the degree of saturation through SWRC, and shown in Figure 9(b). Greater shear modulu were obtained by increasing the suction level. In some cases, the shear modulus drops in suction ranges higher than the one corresponding to the residual water content.

Overall, this form of modulus variation is mostly in accordance with previously reported trends in small-strain shear modulus of unsaturated sand (e.g. Ghayoomi and McCartney 2011) and can be attributed to the expected suction stress pattern in unsaturated sand (Lu et al. 2007). Lu et al. (2010) explained that the stiffness and strength properties of soils are much better correlated with suction stress in comparison

with matric suction. They showed that the suction stress reaches a peak by increasing the matric suction in sands as a result of different interaction mechanisms in air-water-solid interface system. Similarly, this can result in a peak shear modulus (both small-strain and strain-dependent modulus) in unsaturated soils. The noise in the shear modulus data could be associated with experimental data scatter with respect to variation in initial relative density during sample preparation and oscillation in designated pressures that can impact the stiffness and SWRC.

Suction-Dependency of Shear Modulus

The results in Figure 8 can be explained such that the increase in suction while keeping the net normal stress (cell pressure) constant increased the effective stress in the soil. Thus, the higher effective stress within soil specimens resulted in stiffer shear response. In order to eliminate this effect and explore the shear modulus variations independent of the influence of the effective stress, the measured shear moduli were normalized by the square root of the mean effective stress, shown in Figure 10. This normalization method was implemented owing to the common correlation between the shear modulus and the effective stress in sands such as the one in Equation 3. The trend in the results indicated that suction increased the modulus beyond the expected increase due to the higher effective stress. Given the limited available data one can propose a suction (ψ)-dependent shear modulus relation as follows.

$$G = A(OCR)^{K} f(e) \sigma'_{m}^{0.5} f(\gamma) f(\psi)$$
(13)

Strain-Dependent Shear Modulus

As discussed above, it is expected that increasing the induced shear strain level decreases the shear modulus. To validate the consistency of this trend for soils with

different degrees of saturation, the measured shear modulus values were compared for varying shear strain levels under similar suction conditions. The shear modulus versus shear strain plots for dry, saturated, and unsaturated soils with suctions of 2.5, 3, 4.5, and 6 kPa are presented in Figure 11. Similar to what has been reported for dry and saturated soils, the shear modulus decreases nonlinearly, sometimes linear in log-scale plots for this range of strain levels, by increasing the shear strain level. This trend is similar for all suction levels.

Shear-Modulus Reduction Function

In order to better understand the soil behavior under cyclic loading, obtained shear moduli were normalized by the small-strain shear moduli, calculated from the Equation 3 proposed by Seed et al. (1970), and shown in Figure 12. The effects of seating stress in axial direction on the mean effective stress and the effect of suction stress in unsaturated sand on the effective stress attained from Equation 9 were considered in determining the small-strain shear modulus. To compare these data with the available empirical relations for predicting G/G_0 , shear modulus reduction curves were estimated based on the models by Darendeli (2001) (i.e. Eq. 7), Hardin and Drnevich (1972) (i.e. Eqs. 2, 4, and 5), and basic hyperbolic model (i.e. Eqs. 2, 4, and 6) and shown in Figure 12. The mean effective stress and vertical effective stress values in these models were consistently used as the chamber cell pressure (i.e. 50 kPa) to avoid demonstrating several curves. The main purpose was to illustrate these reference curves as a way to verify the pattern and the orders of magnitudes.

The measured values regardless of their saturation level fits well in the range of the curves, especially between the proposed equations by Darendeli (2001) and Hardin and Drnevich (1972). One should consider that these empirical curves are based on numerous

experimental results with considerable scatter (Oztoprak and Bolton 2013). Thus, a perfect match would have not been anticipated. The G/G₀ values for unsaturated soils are different than the ones for dry or saturated soils. This is due to the nonlinear variation of both G and G₀ in dry, unsaturated, and saturated soils. Accordingly, the shear modulus reduction curves for soils shifted up (or in another word shifted to the right) by increasing suction values as a result of their higher shear modulus. The observed modulus variation pattern is consistent with shear modulus curve patterns where higher effective stresses resulted in higher modulus reduction range (e.g. Kramer 1996). Further, Dong et al. (2016) reported that the shear modulus not only depends on the applied stresses but it also depends on the degree of saturation through an inversely proportional relation in sands. Thus, the estimated G₀, solely based on the stress level, may overpredicted the actual G₀, and consequently, resulted in lower G/G₀ ratios. In addition, G₀ values were approximately estimated from an empirical relation that has been developed based on the results from dry sand. Thus, the applied relation may not well represent the response of the tested sand, especially in unsaturated conditions. It should be considered that the suction values for this study are relatively small, so future studies on soils that can retain more water in higher suction would be valuable.

Stress-Control vs. Strain-Control tests

373

374

375

376

377

378

379

380

381

382

383

384

385

386

387

388

389

390

391

392

393

394

395

396

Cyclic triaxial tests can be performed in both strain- and stress-controlled conditions. Stress-controlled tests are more popular due to their simplicity of data analysis and better quality of hysteresis loops. Majority of the tests in this study were performed in strain-controlled condition because of its capability to accurately control the induced shear strain. Strain-controlled experiments with similar strain levels could be executed on sands with different suction values. However, a set of stress-controlled cyclic triaxial tests

were performed on unsaturated sands to compare the results and monitor any inconsistencies that may arise from the testing procedure. After generating the hysteresis stress-strain loops, the induced shear strain and the soil shear modulus were calculated. Then, the normalized shear modulus values (G/G_0) were estimated for stress-controlled tests, and shown alongside the strain-controlled data and empirical relations in Figure 13. The results did not designate any meaningful difference between the two testing methods, indicative of consistent modulus measurement in both tests. The measured modulus from the two testing approaches did not align vertically because the shear strain was measured in stress-controlled tests while it was directly controlled during strain-controlled tests. Although both strain- and stress-controlled tests resulted in relatively similar G/G_0 ratios, they may not fully represent the soil response in pure shear condition. One should note that both empirical relations by Darendeli (2011) and Hardin and Drnevich (1972) are based on data from torsional shear/resonant column tests, which directly simulate shear similar to the field condition. Consequently, careful attention should be given when these curves and triaixial results are used interchangeably.

Conclusions

A cyclic triaxial system was modified for suction-controlled testing to investigate the effect of degree of saturation on strain-dependent shear modulus of unsaturated sand. The study mainly focused on the sand response in medium to large shear strain levels under strain- and stress-controlled sinusoidal loads. The results indicated the shear modulus increased in unsaturated sand by increasing the suction level regardless of the induced strain level. However, this increase was more significant in lower strain range. Additionally, the modulus variation trends were consistent with reported trends for small-strain shear modulus where the modulus starts to decrease after a peak value. By

inspecting the variation of normalized shear modulus with respect to the square root of the effective stress, it is evident that the influence of the effective stress is insufficient to explain the higher shear moduli in unsaturated conditions. Thus, a direct influence of suction could be incorporated in a conceptual suction-dependent shear modulus equation.

By increasing the shear strain in the specimens with similar suction values the modulus decreased nonlinearly. The measured shear moduli (G) were normalized to G_0 values that were predicted from the integration of modulus empirical relations and suction stress-based effective stress formula. The estimated G/G_0 ratios follow a similar hyperbolic trend as predicted by other empirical shear modulus reduction equations. Partially saturated condition led to a shift in shear modulus reduction curves due to a higher effective stress and suction. However, the measured values were mostly lower than the average G/G_0 range estimated from the empirical relation. This could be attributed to the differences in the shear application methods between the empirical formulas and current study and the inability of current formulation to correctly predict G_0 in unsaturated conditions. Further, the results from stress-controlled tests seem to be consistent with the ones from strain-controlled tests limiting the effect of triaxial testing approach on the result. Overall, stress state, inter-particle forces, shearing technique, density, and soil physical properties are the major factors in determining the shear modulus of soils.

Acknowledgement

The authors would acknowledge partial funding of this project by National Science Foundation through the NSF CMMI grant No. 1333810.

REFERENCES

- Alramahi, B., Alshibli, K. A., Fratta, D., Trautwein, S. 2007 "A Suction-Control Apparatus for the
- Measurement of P and S-wave Velocity in Soils", ASTM Geotechnical Testing Journal, 31(1),
- 447 1-12.

- Biglari, M., Jafari, M.K., Shafiee, A., Mancuso, C., and d'Onofrio, A. 2011. "Shear Modulus and
- Damping Ratio of Unsaturated Kaolin Measured by New Suction-Controlled Cyclic Triaxial
- Device", ASTM Geotechnical Testing Journal, 34 (5), 1-12.
- 451 Bishop A.W., 1959, "The principle of effective stress", Tek. Ukeblad, 106(39), 859-863.
- 452 Cary, C. E., Zapata, C. E. 2016 "Pore Water Pressure Response of Soil Subjected to Dynamic
- Loading under Saturated and Unsaturated Conditions" International Journal of
- 454 Geomechanics, online, 1-9.
- 455 Cho, G.C., Santamarina, J.C. 2001 "Unsaturated Particulate Materials—Particle-Level Studies"
- Journal of Geotechnical and Geoenvironmental Engineering, 127 (1), 84-96.
- Cui, Y.J., Tang, A.M., Marcial, D., Terpereau, J.M., Marchadier, G., and Boulay, X. 2007. "Use of
- 458 a Differential Pressure Transducer for the Montoring of Soil Volume Change in Cyclic Triaxial
- Test on Unsaturated Soils.", ASTM Geotechnical Testing Journal, 30(3), 1-7.
- 460 Craciun, O. and Lo, S.-C. R. 2010, "Matric Suction Measurement in Stress Path Cyclic Triaxial
- 461 Testing of Unbound Granular Base Materials", ASTM Geotechnical Testing Journal, 33(1), 1-
- 462 12.
- Darendeli, M. B. 2001. "Development of a new family of normalized modulus reduction and
- 464 material damping curves." PhD dissertation, Univ. of Texas at Austin, Austin, Texas.

- Dashti, S., Bray, J.D., Pestana, J.M., Riemer, M. and Wilson, D. 2010. "Mechanisms of Seismically
- 466 Induced Settlement of Buildings with Shallow Foundations on Liquefiable Soil." Journal of
- Geotechnical and Geoenvironmental Engineering. 136(1), 151-164.
- Dong, Y., McCartney, J. S., Lu, N. 2016 "Small-Strain Shear Modulus Model for Saturated and
- 469 Unsaturated Soil" Go-Chicago 2016, Chicago, pp. 316-325.
- 470 Ghayoomi, M. and McCartney, J.S. 2011. "Measurement of Small-Strain Shear Moduli of Partially
- 471 Saturated Sand during Infiltration in a Geotechnical Centrifuge." ASTM Geotechnical Testing
- 472 Journal, 34(5), 1-12.
- 473 Ghayoomi M., McCartney, J.S., and Ko, H.-Y. 2011 "Centrifuge Test to Assess the Seismic
- 474 Compression of Partially Saturated Sands." ASTM Geotechnical Testing Journal, 34(4), 321-
- 475 331.
- 476 Ghayoomi M., McCartney, J.S., and Ko, H.-Y. 2013 "Empirical Methodology to Estimate
- 477 Seismically Induced Settlement of Partially Saturated Sand" Journal of Geotechnical and
- 478 Geoenvironmental Engineering, Vol. 139, No. 3, pp. 367-376.
- Ghayoomi, M. and Mirshekari, M. 2014, "Equivalent Linear Site Response Analysis of
- 480 Partially Saturated Sand Layers", UNSAT2014 conference, Sydney, Australia, 1-6.
- 481 Hardin, B.O. and Black, W.L. 1969. "Vibration Modulus of Normally Consolidated Clay; Closure."
- 482 J. Soil Mech. Found. Div. ASCE, Vol. 95, SM6, pp. 1531–1537.
- 483 Hardin, B.O., Drnevich, V.P. 1972. "Shear Modulus and Damping in Soils: Design Equations and
- 484 Curves." J. Soil Mech. Found. Div. Proc. ASCE 98, No. SM7, 667–692.
- 485 Hilf, J.W. "An Investigation of Pore-Water Pressure in Compacted Cohesive Soils", Ph.D. Thesis,
- 486 University of Colorado, Boulder, 1956.

- 487 Hoyos, L.R., Suescun-Florez, E.A., and Puppala, A.J. 2015. "Stiffness of Intermediate Unsaturated
- 488 Soil From Simultaneous Suction-Controlled Resonant Column and bender Element Testing."
- 489 Engineering Geology, 188, 10-28.
- 490 Khalili, N., Geiser, F., and Blight, G. E. 2004. "Effective Stress in Unsaturated Soils: Review with
- New Evidence" International Journal of Geomechanics, Vol. 4, No. 2, pp. 115-126.
- 492 Khosravi, A., Ghayoomi, M., and McCartney, J.S. 2010. "Impact of effective stress on the dynamic
- shear modulus of unsaturated sand." GeoFlorida 2010, West Palm Beach, Florida, USA. Feb.
- 494 20-24. CD-ROM.
- 495 Khosravi, A., Salam, S., McCartney, J.S., and Dadashi, A. 2016. "Suction-Induced Hardening
- 496 Effects on the Shear Modulus of Unsaturated Silt" International Journal of Geomechanics,
- 497 online, 1-10.
- 498 Kimoto, S., Oka, F., Fukutani, J., Yabuki, T., and Nakashima, K. 2011. "Monotonic and Cyclic
- Behavior of Unsaturated Sandy Soil under Drained and Fully Undrained Conditions." Soils
- and Foundations, 51(4), 663-681.
- Kokusho, T. 1980. "Cyclic Triaxial Test of Dynamic Soil Properties for Wide Strain Range", Soils
- and Foundations, Vol. 20, No. 2, pp. 45-60
- 503 Kondner, R.L. and Zelasko, J.S. 1963. "Hyperbolic Stress-Strain Formulation for Sands."
- Proceedings, 2nd Pan American Conference on Soil Mechanic and Foundations Engineering,
- 505 289-324.
- 506 Kramer, S.L. 1996. Geotechnical Earthquake Engineering. Prentice Hall, New Jersey.
- 507 Lu N. and Likos W.J., 2006, "Suction stress characteristic curve for unsaturated soil", Journal of
- Geotechnical and Geo-environmental Engineering, Vol. 132, No. 2, 131-142.

- Lu N., Wu, B., and Tan, C.P. 2007. "Tensile Strength Characteristics of Unsaturated Sands." ASCE
- Journal of Geotechnical and Geoenvironmnetal Engineering, 133(2), 144-154.
- 511 Lu, N., Godt, J.W., and Wu, D.T. 2010. "A Closed Form Equation for Effective Stress in
- 512 Unsaturated Soil." Water Resources Research, 46, W05515, 14pp.
- 513 Mancuso, C., Vassallo, R., and d'Onofrio, A. (2002). "Small Strain Behavior of a Silty Sand in
- 514 Controlled-Suction Resonant Column-Torsional Shear Tests." Canadian Geotechnical
- 515 Journal. CGJ. Vol. 39, No. 1, 22-31.
- Marinho, E.A.M., Chandler, R.J., and Crilly, M.S. 1995. "Stiffness Measurements on an
- 517 Unsaturated High Plasticity Clay using Bender Elements." Proc. of the First International
- 518 Conference on Unsaturated Soils, UNSAT '95, Paris, France, 6–8 September 1995. A.A.
- Balkema, Rotterdam, the Netherlands. Vol. 2. 535–539.
- 520 Mendoza, C.E., Colmenares, J.E., and Merchan, V.E. (2005). "Stiffness of an Unsaturated
- 521 Compacted Clayey Soil at Very Small Strains." Conf. on Advanced Experimental Unsaturated
- 522 Soil Mechanics. Trento, Italy. 27-29 June. 199-204.
- Meng, F.-Y., 2003. "Dynamic Properties of Sandy and Gravelly Soils", PhD Thesis, the University
- of Texas at Austin.
- 525 Mirshekari, M. and Ghayoomi, M. (2015), "Simplified Equivalent Linear and Nonlinear Site
- Response Analysis of Partially Saturated Soil Layers", IFCEE 2015, Geotechnical Special
- Publication 256, M. Iskander, M.T. Suleiman, J.B. Anderson, D.F. Laefer eds., San Antonio,
- 528 Texas, 2131-2140.
- 529 Ng, C.W.W., Xu, J. and Yung, S.Y. 2009. "Effects of imbibition-drainage and stress ratio on
- anisotropic stiffness of an unsaturated soil at very small strains." Canadian Geotechnical
- 531 Journal, Vol. 46, No. 9, 1062-1076.

Oztoprak, S. and Bolton, M.D. "Stiffness of Sands through a laboratory test database", 532 Geotechnique, 63(1), 54-70. 533 Seed, R. B., & Duncan, J. M. 1986. "FE analyses: compaction-induced stresses and deformations." 534 Journal of Geotechnical Engineering, 112(1), 23-43. 535 Seed, H.B. and Idriss I.M. 1970. "Soil Moduli and Damping Factors for Dynamic Response 536 Analyses." Rep. No. EERC70-10. Earthquake Eng. Res. Ctr., Univ. of California, Berkeley, 537 538 Calif. van Genuchten, M. 1980. A Closed Form Equation for Predicting the Hydraulic Conductivity of 539 540 Unsaturated Soils." Soil Sci. Soc. Am. J., 58, 647-652.

541	List of Figure Captions
542	
543	Figure 1. (a) Cyclic hysteresis stress-strain relationship; (b) Cyclic backbone curve (after Kramer 1996)
544	Figure 2. Modulus reduction (after Kramer 1996)
545	Figure 3. Modified triaxial system at University of New Hampshire
546	Figure 4. Grain-size distribution for Ottawa F-75
547	Figure 5. Soil-water retention curve for Ottawa F75 sand
548	Figure 6. Cyclic Hysteresis Loops for: (a) Regular cases; (b) Soft extension cases; (c) Hardening in stress
549	controlled test; (d) Softening cases
550	Figure 7. Suction variation during cycles of dynamic triaxial testing
551	Figure 8. Shear modulus variation examples during cycles of dynamic triaxial testing
552	Figure 9. Effect of (a) degree of saturation and (b) suction on dynamic shear modulus
553	Figure 10. Effect of suction on normalized dynamic shear modulus with respect to the initial mean
554	effective stress
555	Figure 11. Effect of shear strain level on dynamic shear modulus of dry, saturated, and unsaturated sand
556	Figure 12. Normalized shear modulus reduction values for strain-controlled test compared with empirical
557	equations.
558	Figure 13. Normalized shear modulus reduction values in strain- and stress-controlled tests

<u>Input Parameter</u>	<u>Value</u>
Coefficient of curvature, C _c	1.71
Coefficient of uniformity, Cu	1.01
Specific gravity, Gs	2.65
D ₅₀ (mm)	0.182
Dry density limits, ρ _{d-min} , ρ _{d-max} (kg/m ³)	1469, 1781
Void ratio limits, e _{min} , e _{max}	0.49, 0.80
Relative density, D _r	0.45
Friction angle (deg)	40
Poisson's ratio, υ	0.38
van Genuchten's a _{vG} parameter (kPa ⁻¹)	0.25
van Genuchten's N _{vG} parameter	9
Residual volumetric water content, θ_r	0.07
Saturated volumetric water content, θ_s	0.39

Table 2. Experimental Plan

562

Test Type	Suction (kPa)	Degree of Saturation	Shear Strain (%)
		(%)	
Strain Control	0	0	0.069, 0.14, 0.28, 0.69
	0	100	0.014, 0.028, 0.069, 0.14, 0.28
	2	99.8	0.069
	2.5	98.9	0.014, 0.028, 0.28, 0.69
	3	94.9	0.069, 0.14, 0.28, 0.55
	3.5	83.0	0.069, 0.14, 0.28, 0.69
	4	62.4	0.069, 0.14, 0.28
	4.5	42.8	0.028, 0.14, 0.28, 0.69
	6	21.5	0.069, 0.14, 0.28, 0.69, 1.10
	8	18.7	0.14, 0.28, 0.69
	10	18.4	0.14, 0.28, 1.38
	2.5	98.9	0.31, 0.33, 0.50
Stress Control	3.5	83	0.11,0.15, 0.21
	4.5	42.8	0.12, 0.19, 0.26
	6	21.5	0.04, 0.09, 0.13, 0.26
	8	18.7	0.19, 0.24, 0.34

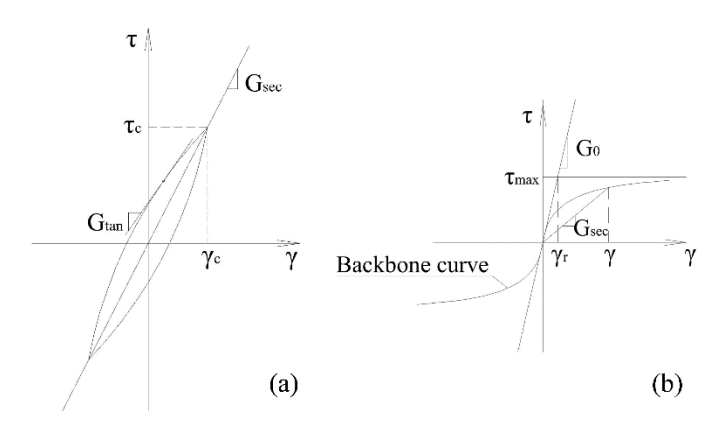
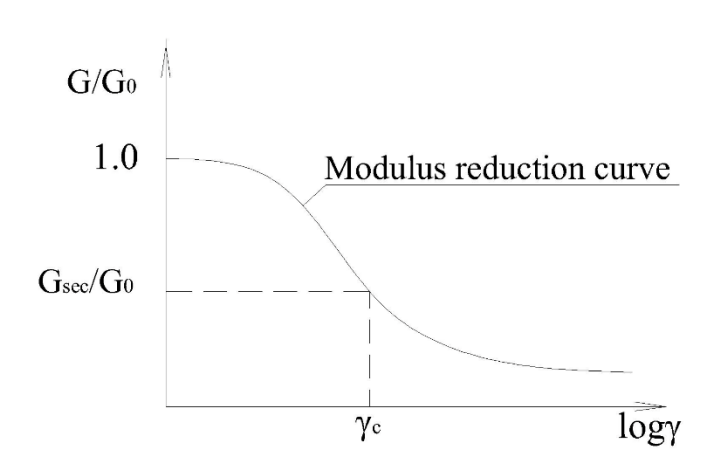
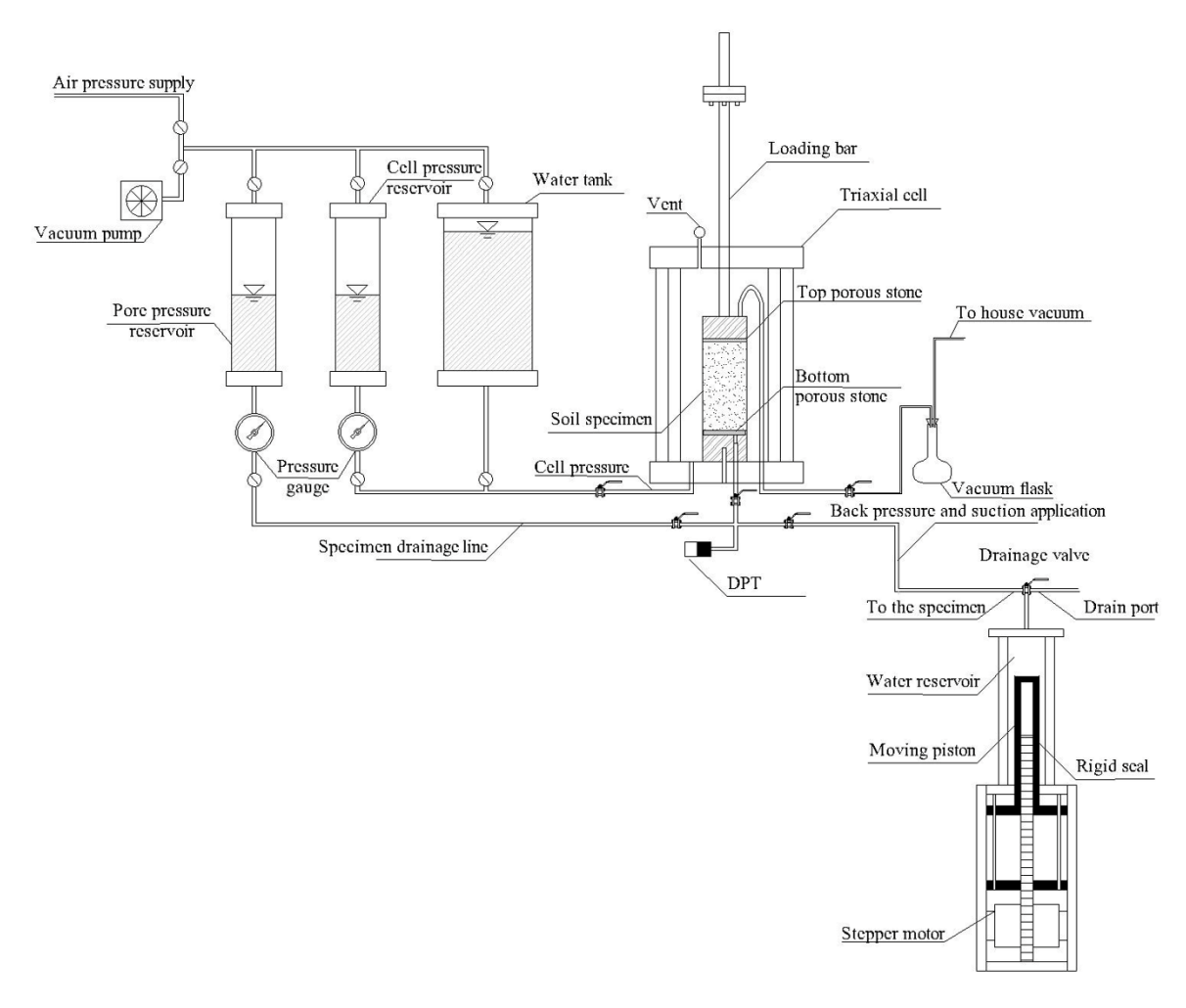


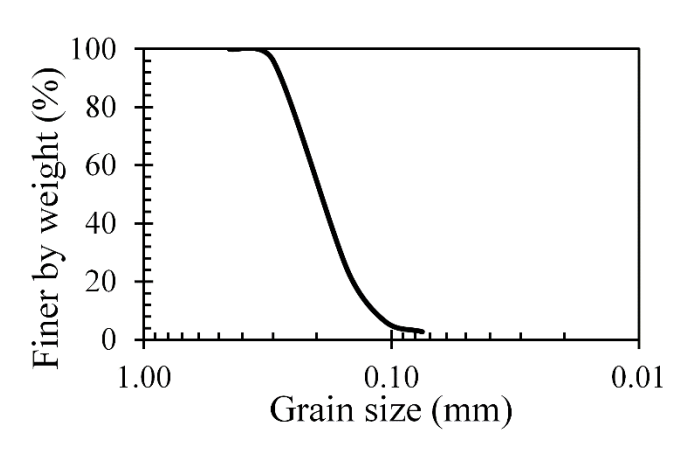
Figure 1.



571 Figure 2.



573 Figure 3.



576 Figure 4.

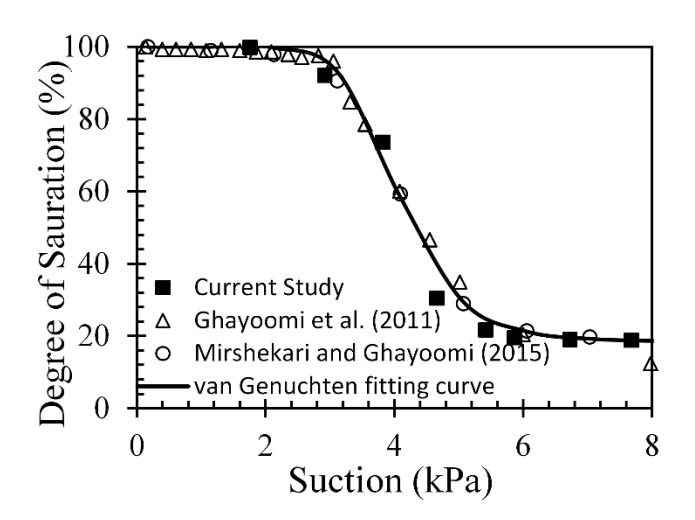
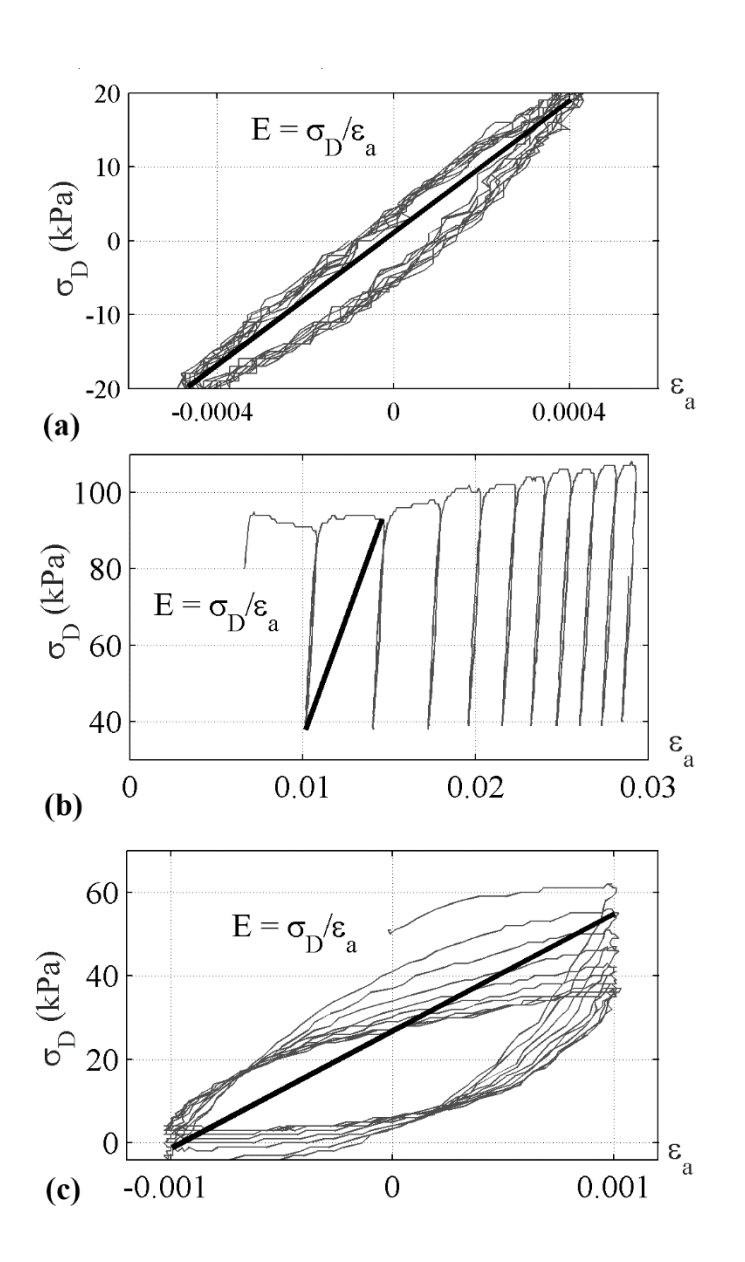
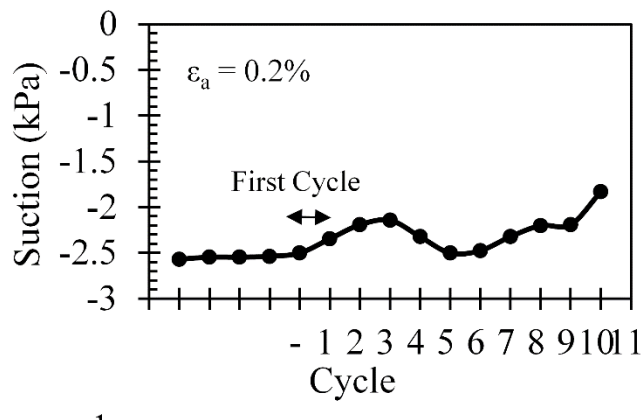
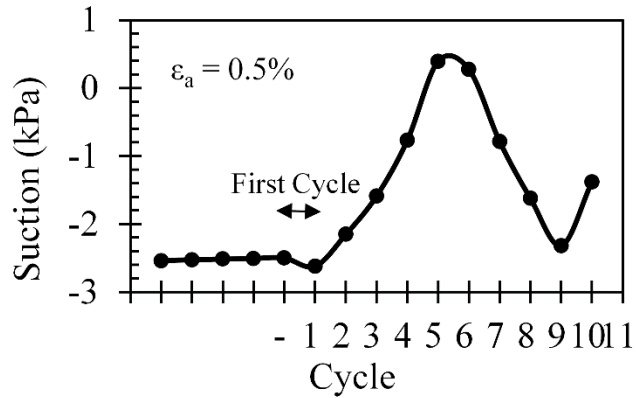


Figure 5.



582 Figure 6.

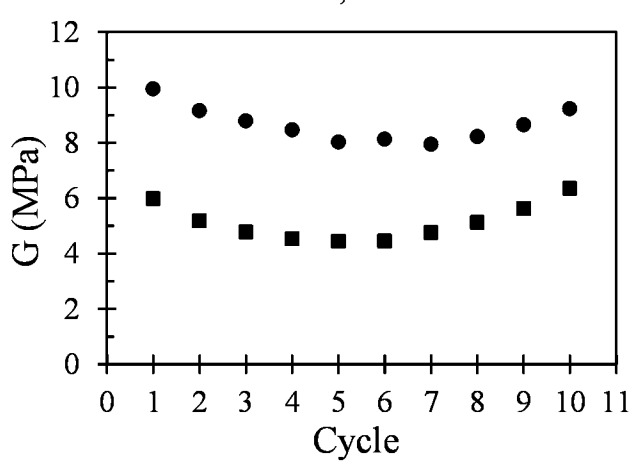




584 585 Figure 7.

• Suction = 2.5 kPa, Axial Strain = 0.2%

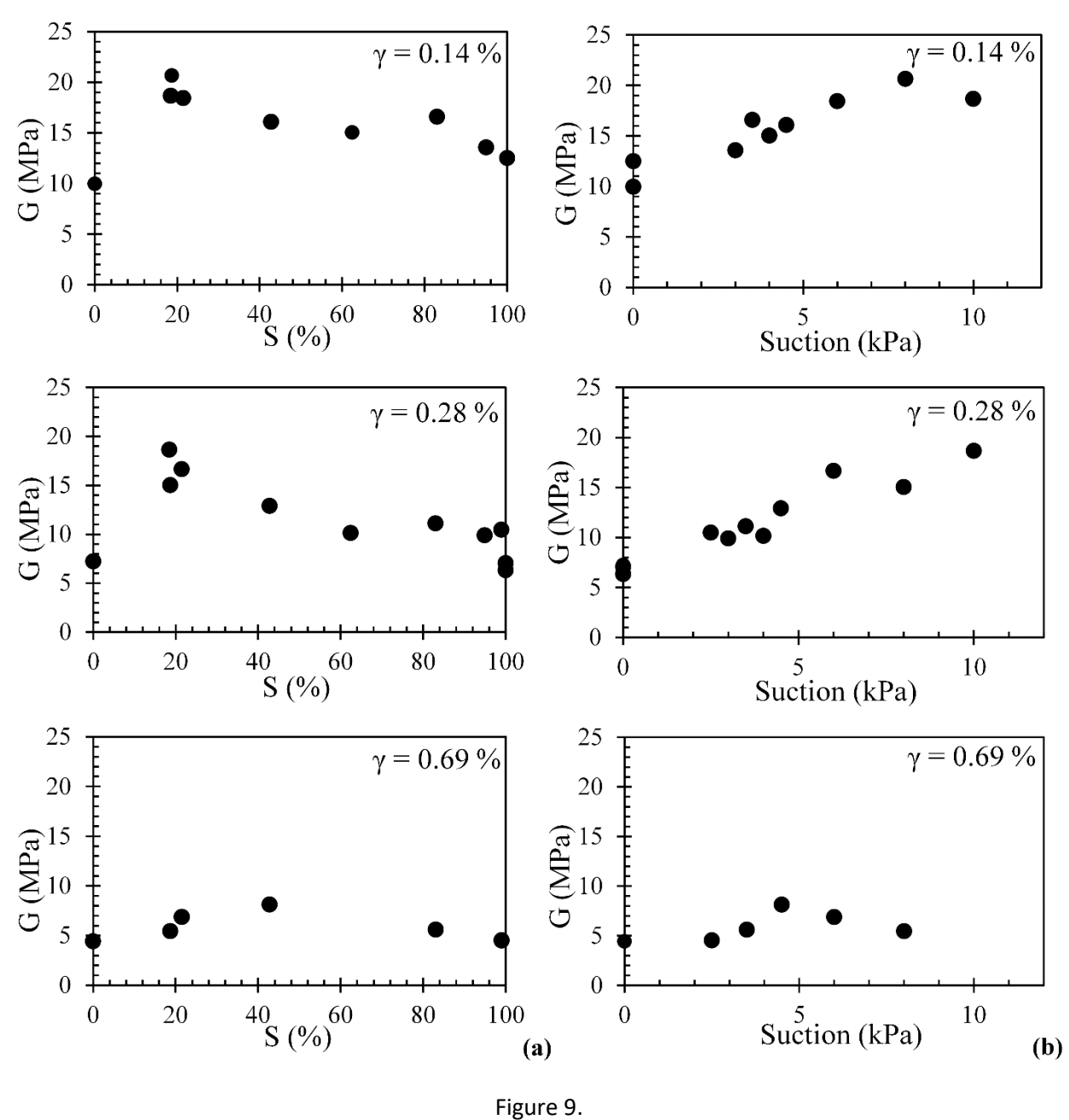
■ Suction = 2.5 kPa, Axial Strain = 0.5%

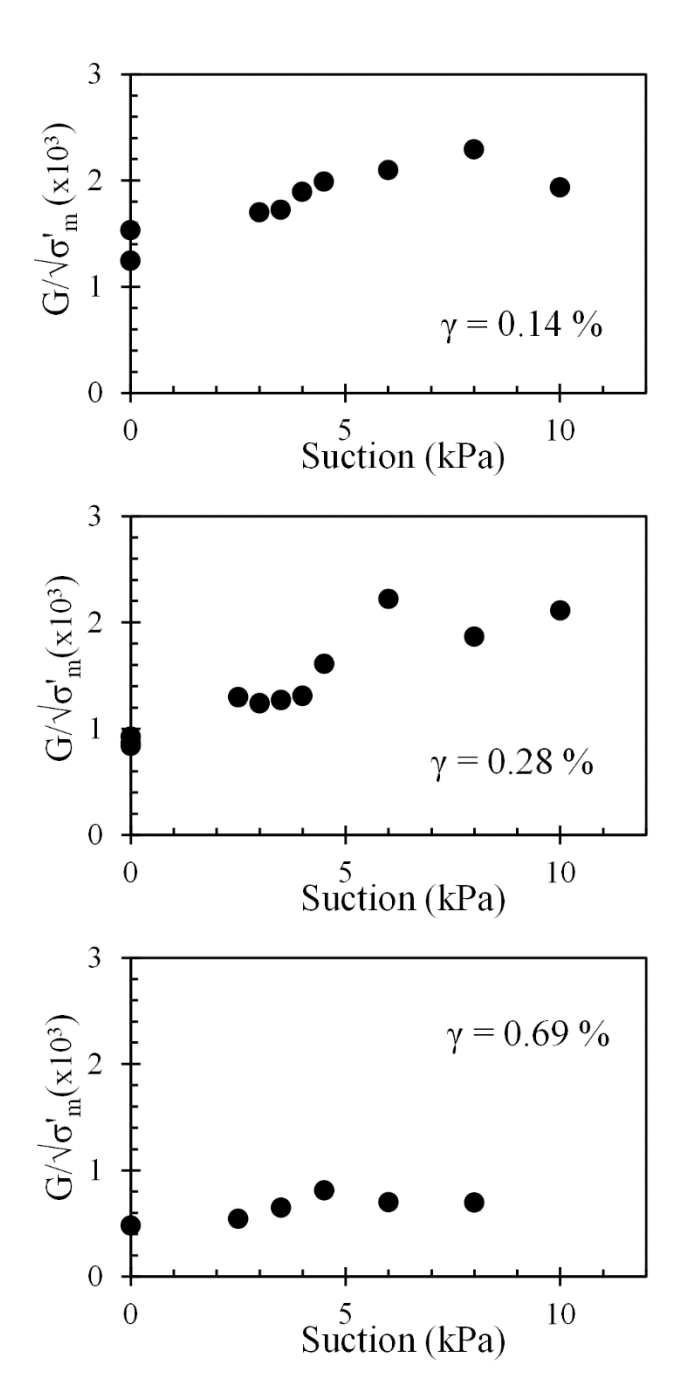


586

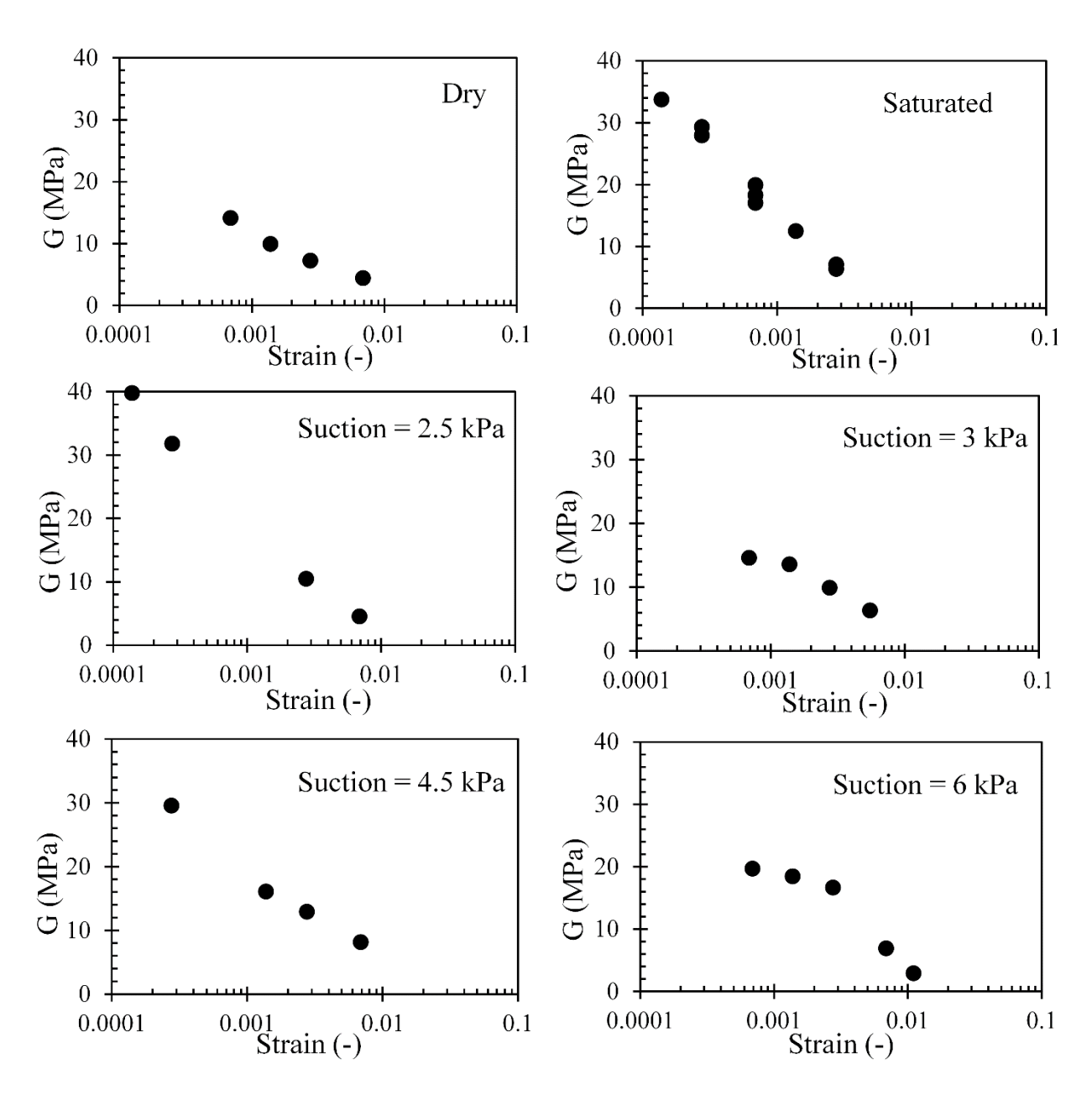
587

Figure 8.





591 Figure 10.



593 Figure 11.

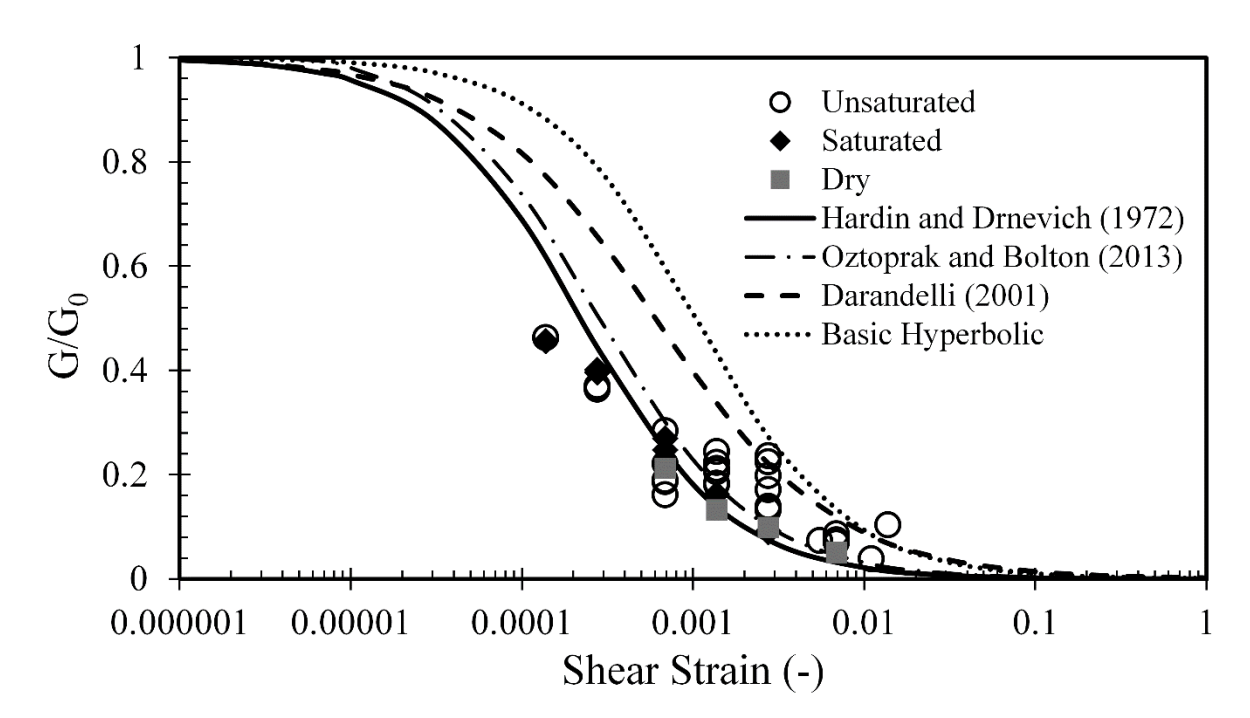


Figure 12.

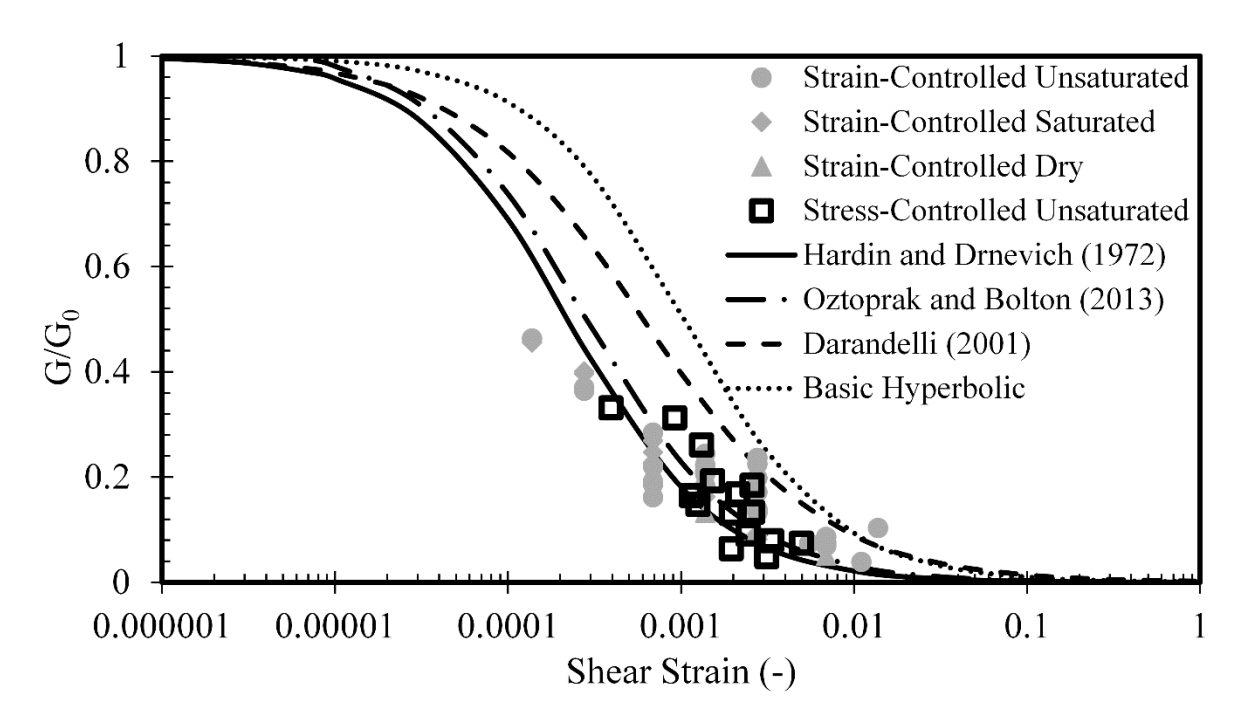


Figure 13.